



LUND UNIVERSITY
Faculty of Science

Model study of the linear density response function - A comparison between the exact result and RPA

Viktor Christiansson

Thesis submitted for the degree of Bachelor of Science
Project duration: 2 months

Supervised by Prof. Ferdi Aryasetiawan

Department of Physics
Division of Mathematical Physics
May 2017

Abstract

The time-ordered linear density response function is examined in a model study. Two model dimers are considered; one with one orbital per site and a second one with two orbitals per site. The one-orbital case has U_0 , the on-site Coulomb interaction, as the only parameter and is solved analytically. The two-orbital case has parameters U_0 , the upper orbital non-interacting eigenenergy ε_1 , and the hopping terms t and t' and is solved numerically. The response function is calculated within the Random-Phase Approximation (RPA) and is compared to the exact results for varied parameters. The general trends found in the study are that RPA seems to get worse for increasing U_0 due to the increased localization, and improves for increasing t' attributed to the increase in delocalization. Furthermore, the two-orbital case was seen to reduce to the on-orbital one for increasing ε_1 and in the limit of small t' , which can be used as an analytical check for the correctness of the two-orbital model as it reduces to the one-orbital case which was solved analytically.

Teoretisk modellering: hur vi beskriver verkligheten

Att veta hur något kommer att svara på en handling är viktig information att ha, inom fysiken liksom i vardagen. Medan den mer vanliga typen av handling-respons kanske handlar om att veta om ett föremål går sönder om jag råkar tappa det, så är responsen man tittar på inom materialfysik snarare relaterat till hur någonting utifrån kommer att påverka materialet. Att beräkna denna påverkan är däremot oftast svår, om inte omöjlig, men vi är inte desto mindre intresserade av att beräkna den. Istället har ungefärliga metoder utvecklats, men för att dessa metoder ska kunna användas för riktiga experiment så måste det först fastslås hur bra denna förenklade metod verkligen överensstämmer med verkligheten.

Ett exempel på hur omvärlden kan påverka ett material är helt enkelt genom att skina ljus på det. Detta påverkar elektronerna som åker runt inuti och kan, beroende på ljuset, ha olika effekter på elektronerna. De kan antingen *exciteras*, få mer energi, eller flyga ut ur materialet. Det senare är den typ av experiment som görs på det nyöppnade MAX IV i Lund där de utkastade elektronerna kan användas för att bestämma egenskaper hos materialet, vilket visar på vikten som läggs på den här typen av forskning.

Eftersom den här typen av experiment bevisligen blir mycket dyr är det inte alltid möjligt att undersöka allt som hade önskats. Däremot så kan effekten av den yttre påverkan även räknas ut, kanske inte med papper och penna, men åtminstone en dator. Det kan därför kanske verka perfekt att bara kunna skriva ett litet program och få reda på allt vi någonsin skulle kunna drömma om att veta om materialet i fråga, men dessvärre är det inte så enkelt. Detta beror på den enorma storleken på problemet med ett ofattbart antal elektroner som inte bara påverkas av det yttre utan även interagerar med varandra. Så hur kan man lösa detta? Istället för att titta på ett riktigt material används modeller, som får representera det verkliga problemet, och approximationer som förenklar de inblandade faktorerna. Om då en tillräckligt enkel modell, som representerar en verklig fysisk situation, används, är det möjligt att exakt beräkna vad effekten blir. Genom att jämföra detta med den förenklade approximationen och se ifall de två ger samma svar är det möjligt att se hur denna approximativa metod fungerar. I sin tur ger det oss möjligheten att få information om vad vi kan förvänta oss när vi gör beräkningarna för riktiga material: hur väl överensstämmer vår matte egentligen med verkligheten?

Acknowledgements

I would like to express my deep gratitude to my supervisor Professor Ferdi Aryasetiawan for his continued support, guidance and commitment during my Bachelor thesis. I greatly appreciate the time he has spent on helping me and the advise he has provided throughout my work.

Contents

1	Introduction	1
2	Theory and Method	3
2.1	The Model	3
2.2	Response Function	4
2.3	Random-Phase Approximation	5
2.4	Exact solution of R	6
2.5	Exact solution for RPA	9
2.6	Numerical solution of R	11
2.7	Numerical solution for RPA	12
3	Results	15
3.1	One-orbital	15
3.2	Two-orbital	16
4	Conclusion	22
5	Outlook	25
	Appendix A Occupation number representation	26
	References	28

Acronyms

RPA - Random-phase approximation

LAPACK - Linear algebra package

1 Introduction

The time-ordered linear charge density response function R [1, 2], hereafter called response function, defined in section 2.2, is a quantity enabling the calculation of the change in the electron density due to the presence of an external perturbing field for many-electron systems. Furthermore, R is a property of the system and is as such independent of the external field. Knowledge of it can be used for example to find the exact excitation spectra of the many-electron system, the response to photo-emission experiments used to discover properties of materials and also for computing the screened interaction W given schematically by $W = v + vRv$ where v is the non-screened Coulomb interaction [3].

The screened interaction is in turn important for calculating the Green's function G of the many-electron system which, for example, can be used to calculate the self-energy within the GW approximation. The interacting Green's function can then be computed using the Dyson equation [3]. In the present study the focus will be on the excitation energies and the self-energy will not be studied at all.

Due to the large difficulty of computing the exact response function in a real system, approximations must be used in order to make progress. One such approximation, which has been highly successful, is the random-phase approximation (RPA) developed by Bohm and Pines [4] in the 1950s during their work on collective excitations in the electron gas. They derived it using the equation of motion method and the "random-phase" relates back to terms which are neglected due to that their random phases cancels out. Later, Gell-Mann and Brueckner [5] showed that the result can also be found using the many-body diagrammatic perturbation theory technique. Since then it has been understood that RPA can be seen as a time-dependent Hartree approximation where only the change in the Hartree potential due to the induced density from the perturbing external field is considered [1].

The RPA works well for systems with delocalized electrons [1], usually materials with s or p valence electrons; however, more localized systems with partially filled $3d$ or $4f$ orbitals with interesting properties have been discovered. These materials include, for example, high-energy superconductors, and perovskite materials which are showing promise for use in solar cells [6]. Moreover, RPA is not expected to be good for these localized systems and as such the question arises when RPA starts to become unreliable.

This study attempts to address the issue by studying two models of hydrogen dimers (two sites), one with an orbital on each site and one with two orbitals per site, for which the exact response function can be calculated. Two electrons in the singlet configuration are considered and a Coulomb interaction (the Hubbard U) to penalize the presence of two electrons on the same orbital is introduced and can be considered a measure of the strength of correlations,

as will be discussed in section 4. Furthermore, the unit used throughout the study is that of the hopping term between the lower orbitals, t , to be introduced in the subsequent section.

The one-orbital case can be solved analytically and therefore also serves as a check for the two-orbital case, which is solved numerically. Both the exact response function and that within RPA are calculated for different parameter values in order to determine in what regime RPA begins to deviate significantly from the exact one.

2 Theory and Method

2.1 The Model

To represent the states used in the model the occupation number representation formalism is used. A short summary of what is needed is provided in appendix A.

Two different systems of a hydrogen dimer will be considered in this work; a dimer with one orbital on each of the two sites and an expanded system with two orbitals on each site. The model Hamiltonian used for both cases is a Hubbard Hamiltonian [7] of the form

$$H = \sum_{i,j} \sum_{\sigma} \langle i | h_0 | j \rangle c_{i\sigma}^{\dagger} c_{j\sigma} + \frac{1}{2} \sum_{i,j,k,l} \sum_{\sigma,\sigma'} \langle ij | v | kl \rangle c_{i\sigma}^{\dagger} c_{j\sigma'}^{\dagger} c_{l\sigma'} c_{k\sigma} \quad (1)$$

where $|i\rangle$ are the one-particle basis states, $h_0 = -\frac{1}{2}\nabla^2 + v_{ext}$ is the non-interacting part of the Hamiltonian with v_{ext} being an external potential, and $v(\mathbf{r}, \mathbf{r}')$ is the effective Coulomb interaction between two electrons located at \mathbf{r} and \mathbf{r}' respectively. c_i^{\dagger} and c_i are the creation and annihilation operators associated with orbital i as defined in appendix A.

The matrix elements will be considered the parameters of the system with the notations $\langle i | h_0 | j \rangle = h_{ij}$ and $\langle ij | v | kl \rangle = U_{ijkl}$. The number of parameters will be constrained due to the limited scope of the work and will be chosen depending on which are more likely to have an influence from a physical perspective. The assumption is made that only on-site intra-orbital Coulomb interaction will occur, which will be justified later. The Hamiltonian can therefore be reduced to

$$H = \sum_{i,j} \sum_{\sigma} h_{ij} c_{i\sigma}^{\dagger} c_{j\sigma} + \frac{1}{2} \sum_i \sum_{\sigma,\sigma'} U_{iiii} c_{i\sigma}^{\dagger} c_{i\sigma'}^{\dagger} c_{i\sigma'} c_{i\sigma} \quad (2)$$

and introducing $n_k = c_i^{\dagger} c_i$, which counts the occupation of k in the state it operates on, the Hamiltonian can be rewritten as

$$H = \sum_{i,j} \sum_{\sigma} h_{ij} c_{i\sigma}^{\dagger} c_{j\sigma} + \sum_i U_{iiii} n_{i\uparrow} n_{i\downarrow}. \quad (3)$$

In the first dimer with only one orbital per site, $i, j = 1, 2$, the Coulomb interaction parameters U_{1111} and U_{2222} will be the same as the two states are interchangeable and a common on-site Coulomb interaction parameter $U_{1111} = U_{2222} = U_0$ can be set. The h_{11} and h_{22} terms correspond to the non-interacting eigenenergies for the two sites and they can be written $h_{11} = h_{22} = \varepsilon_0$ and may be set to zero. Finally, the creation and annihilation operators associated with h_{12} and h_{21} correspond to annihilating an electron on one site and creating it on the other which describes the electron hopping between the two sites.

Therefore, $h_{12} = h_{21} = t$ is the hopping term.

In the second system with two orbitals on each site, the lowest orbitals are denoted $i, j = 1$ and 2, and the upper ones $i, j = 3$ and 4 for the two sites respectively. As before the upper and lower states have their respective non-interacting eigenenergies and the parameters can therefore be set as $h_{11} = h_{22} = \varepsilon_0$ and $h_{33} = h_{44} = \varepsilon_1$. The lower states also have on-site Coulomb interaction given by U_0 , however, the two upper states can be considered as a reservoir containing all the excited states of a real system. The model is generic of strongly correlated materials with localized electrons in the valence band whereas the other higher states are delocalized, whereupon U_{3333} and U_{4444} are set to 0.

The inclusion of these reservoir states allows for additional fluctuations of the electron density as hopping is allowed between additional states. To limit the problem only the hopping terms $h_{12} = h_{21} = t$ and $h_{14} = h_{41} = h_{23} = h_{32} = t'$, which are thought to be the most important, are included. Furthermore, the on-site hopping terms h_{13} and h_{24} can be effectively included in the orbital energies ε_0 and ε_1 and need not be considered individually.

By setting $t' = 0$ there should not be any coupling between the lower and upper states and the extended system should reduce to the one-orbital case. Consequently, this allows for comparison between the cases and the different approaches used to solve them: analytically for the one-orbital case and numerically for the two-orbital case.

2.2 Response Function

The time-ordered linear charge density response function provides the ability to calculate the linear change in density due to applying an external field on the system and is calculated as

$$R(rt, r't') = \frac{\delta\rho(r, t)}{\delta\varphi(r', t')} \quad (4)$$

where $\rho(r, t)$ is the density at the position r and time t , and $\varphi(r', t')$ is the external field which is applied at the position r' and time t' . Here the notation $r = (\mathbf{r}, \sigma)$ also includes the spin.

It can be shown that the spectral representation of the response function is given by [2, 3]

$$R(r, r'; \omega) = \sum_n \left[\frac{\langle \Psi | \hat{\rho}(r') | n \rangle \langle n | \hat{\rho}(r) | \Psi \rangle}{\omega - E_n + E_0 + i\eta} - \frac{\langle \Psi | \hat{\rho}(r) | n \rangle \langle n | \hat{\rho}(r') | \Psi \rangle}{\omega + E_n - E_0 - i\eta} \right] \quad (5)$$

if the sum is only taken over the excited states, where $|\Psi\rangle$ is the ground state with energy E_0 and $|n\rangle$ are the excited states with energies E_n found by diagonalizing the Hamiltonian in equation (3), and η is an introduced Lorentzian broadening. $\hat{\rho}(r) = \hat{\psi}^+(r)\hat{\psi}(r)$ is the density operator with, in occupation number representation, $\hat{\psi}^+(r) = \sum_i \phi_i^*(r)c_i^+$ and $\hat{\psi}(r) =$

$\sum_j \phi_j(r) c_j$ being the field operators where ϕ_i are orbitals.

The real part of the response function is obtained setting $\eta = 0$ and the spectral function can be calculated as

$$S(\omega) = -\frac{1}{\pi} \text{sgn}(\omega) \text{Im}(R(\omega)) \quad (6)$$

and will give the excitation spectrum of the system and provides all information as

$$R(r, r'; \omega) = \int_0^\infty d\omega' S(r, r'; \omega') \left[\frac{1}{\omega - \omega' + i\eta} - \frac{1}{\omega + \omega' - i\eta} \right] \quad (7)$$

The f-sum rule [1] is a system dependent quantity which states

$$\int d\omega \omega S(\omega) = cN \quad (8)$$

where N is the number of particles and c is a system dependent constant. Using a Lorentzian broadening of $S(\omega)$ will cause the integral to numerically diverge, since

$$R(\omega) \propto \frac{1}{\omega - E_n + E_0 + i\eta} = \frac{\omega - E_n + E_0 - i\eta}{(\omega - E_n + E_0 + i\eta)(\omega - E_n + E_0 - i\eta)} \quad (9)$$

and $S(\omega)$ is by equation (6) proportional to $\text{Im}(R(\omega))$ which for large ω goes as $1/\omega^2$. Thus, the integrand in equation (8) will behave like $1/\omega$, for which the integral numerically diverges. So, in order to compare the results with RPA (to be explained below) a cut-off region can be chosen and the sum rule compared within this interval.

2.3 Random-Phase Approximation

The Random-Phase Approximation (RPA) [1, 2, 4] is used to approximate the response function by taking into account the Hartree potential arising from the induced density. Although, the system itself is considered a non-interacting one. Schematically the linear response of the density then becomes, using equation (4)

$$\delta\rho = R^{\text{RPA}} \delta\varphi = P^0(\delta\varphi + \delta V_H), \quad (10)$$

where P^0 is the polarisation function and is the response of the non-interacting system to the total field $\varphi + V_H$. It is given by [3]

$$P^0(r, r'; \omega) = -2i \int_{-\infty}^{\infty} \frac{d\omega'}{2\pi} G^0(r, r'; \omega + \omega') G^0(r', r; \omega') \quad (11)$$

in frequency space with the 2 coming from the spin and can be solved using contour integra-

tion. $G^0(r, r'; \omega)$ is the non-interacting Green's function of the system

$$G^0(r, r'; \omega) = \sum_i^{\text{occ}} \frac{\psi_i(r)\psi_i^*(r')}{\omega - \epsilon_i - i\eta} + \sum_j^{\text{unocc}} \frac{\psi_j(r)\psi_j^*(r')}{\omega - \epsilon_j + i\eta} \quad (12)$$

with ϵ_i being the eigenvalue corresponding to the eigenstate ψ_i giving P^0 to be

$$P^0(r, r'; \omega) = \sum_i^{\text{occ}} \sum_j^{\text{unocc}} \psi_i(r)\psi_j(r)\psi_i(r')\psi_j(r') \left[\frac{1}{\omega - \epsilon_j + \epsilon_i + i\eta} - \frac{1}{\omega + \epsilon_j - \epsilon_i - i\eta} \right]. \quad (13)$$

Equation (10) can be rewritten using that $\delta V_H / \delta \rho = v$

$$R^{\text{RPA}} \delta \varphi = P^0 (\delta \varphi + v \delta \rho) \quad (14)$$

which after using equation (4) again and as φ is arbitrary yields

$$R^{\text{RPA}} = P^0 + P^0 v R^{\text{RPA}}. \quad (15)$$

This can be written more formally as the RPA equation

$$R^{\text{RPA}}(r, r'; \omega) = P^0(r, r'; \omega) + \int dr_1 dr_2 P^0(r, r_1; \omega) v(r_1 - r_2) R^{\text{RPA}}(r_2, r'; \omega) \quad (16)$$

2.4 Exact solution of R

The one orbital per site case is limited enough for an analytical solution to be possible which will be outlined here for the case of two electrons in the singlet configuration. The four possible configurations for the singlet case which will be considered as the basis states are defined as

$$\begin{aligned} |1\rangle &= c_{1\uparrow}^+ c_{2\downarrow}^+ |0\rangle = |\uparrow \cdot \downarrow\rangle \\ |2\rangle &= c_{1\downarrow}^+ c_{2\uparrow}^+ |0\rangle = |\downarrow \cdot \uparrow\rangle \\ |3\rangle &= c_{1\uparrow}^+ c_{1\downarrow}^+ |0\rangle = |\uparrow \downarrow \cdot\rangle \\ |4\rangle &= c_{2\uparrow}^+ c_{2\downarrow}^+ |0\rangle = |\cdot \uparrow \downarrow\rangle \end{aligned}$$

using the notation $|\text{Site1} \cdot \text{Site2}\rangle$ for the states. The Hamiltonian of the system is, using equation (3) and the parameters defined in section 2.1,

$$H = \begin{pmatrix} \varepsilon_0 & 0 & t & t \\ 0 & \varepsilon_0 & -t & -t \\ t & -t & \varepsilon_0 + U_0 & 0 \\ t & -t & 0 & \varepsilon_0 + U_0 \end{pmatrix}$$

By setting $\varepsilon_0 = 0$ and solving the eigenvalue problem the eigenstates v_1, v_2, v_3 and v_4 can be found in vector form to be

$$v_1 = \begin{pmatrix} -y \\ y \\ x \\ x \end{pmatrix} \quad v_2 = \frac{1}{\sqrt{2}} \begin{pmatrix} 1 \\ 1 \\ 0 \\ 0 \end{pmatrix} \quad v_3 = \frac{1}{\sqrt{2}} \begin{pmatrix} 0 \\ 0 \\ 1 \\ -1 \end{pmatrix} \quad v_4 = \begin{pmatrix} x \\ -x \\ y \\ y \end{pmatrix}$$

with the conditions $2x^2 + 2y^2 = 1$ and $x = 2yt/\epsilon_4$. The eigenenergies for the states are $\epsilon_1 = \frac{1}{2}(U_0 - \sqrt{U_0^2 + 16t^2})$, $\epsilon_2 = 0$, $\epsilon_3 = U_0$ and $\epsilon_4 = \frac{1}{2}(U_0 + \sqrt{U_0^2 + 16t^2})$. The eigenstates $|v_i\rangle$ are used to solve equation (5), with $|v_1\rangle = |\Psi\rangle$ being the ground state, and can be expanded as

$$|v_1\rangle = -y|1\rangle + y|2\rangle + x|3\rangle + x|4\rangle \quad (17)$$

$$|v_2\rangle = \frac{1}{\sqrt{2}}(|1\rangle + |2\rangle) \quad (18)$$

$$|v_3\rangle = \frac{1}{\sqrt{2}}(|3\rangle - |4\rangle) \quad (19)$$

$$|v_4\rangle = x|1\rangle - x|2\rangle + y|3\rangle + y|4\rangle \quad (20)$$

The eigenstates $|v_i\rangle = |\Psi\rangle, |n\rangle$ can in general be expanded as $\sum_k b_k^{v_i} |k\rangle$ with $b_k^{v_i}$ being the expansion coefficient for $|v_i\rangle$ in basis state $|k\rangle$. The matrix elements in equation (5) can then in general be written as

$$\langle \Psi | \hat{\rho}(r) | n \rangle = \left(\sum_k b_k^\Psi \langle k | \right) \sum_{i,j} c_i^+ c_j \phi_i(r) \phi_j(r) \left(\sum_l b_l^n | l \rangle \right) \quad (21)$$

assuming real orbitals ϕ_i and real expansion coefficients. Matrix elements of the form $\langle k | c_i^+ c_j | l \rangle$ must thus be evaluated which is done using the anticommutation relations between the annihilation and creation operators, $\{c_i^+, c_j^+\} = \{c_i, c_j\} = 0$ and $\{c_i^+, c_j\} = \delta_{ij}$, as given in appendix A, in the following way

$$\begin{aligned}
\langle k | c_i^+ c_j | l \rangle &= [k, l = 1, i, j = 1 \uparrow] = \langle 0 | c_{2\downarrow} c_{1\uparrow} c_{1\uparrow}^+ c_{1\uparrow} c_{1\uparrow}^+ c_{2\downarrow}^+ | 0 \rangle = \\
&= \langle 0 | c_{2\downarrow} c_{1\uparrow} c_{1\uparrow}^+ (1 - c_{1\uparrow}^+ c_{1\uparrow}) c_{2\downarrow}^+ | 0 \rangle = \\
&= \langle 0 | c_{2\downarrow} c_{1\uparrow} c_{1\uparrow}^+ c_{2\downarrow}^+ | 0 \rangle - \langle 0 | c_{2\downarrow} c_{1\uparrow} c_{1\uparrow}^+ c_{1\uparrow}^+ c_{1\uparrow} c_{2\downarrow}^+ | 0 \rangle = \\
&= \langle 0 | c_{2\downarrow} (1 - c_{1\uparrow}^+ c_{1\uparrow}) c_{2\downarrow}^+ | 0 \rangle - \langle 0 | c_{2\downarrow} c_{1\uparrow} c_{1\uparrow}^+ c_{1\uparrow}^+ (-c_{2\downarrow}^+ c_{1\uparrow}) | 0 \rangle = \\
&= \langle 0 | c_{2\downarrow} c_{2\downarrow}^+ | 0 \rangle - \langle 0 | c_{2\downarrow} c_{1\uparrow}^+ c_{1\uparrow} c_{2\downarrow}^+ | 0 \rangle + 0 = \\
&= \langle 0 | (1 - c_{2\downarrow}^+ c_{2\downarrow}) | 0 \rangle + 0 = \langle 0 | 0 \rangle = 1
\end{aligned}$$

To find the complete matrix elements all possible permutations of k, l and i, j are done in a similar way as above with all the non-zero combinations given in Table 1.

Table 1: The non-zero matrix elements used to calculate the response function.

$\langle 1 c_{1\uparrow}^+ c_{1\uparrow} 1 \rangle = 1$	$\langle 1 c_{2\downarrow}^+ c_{2\downarrow} 1 \rangle = 1$	$\langle 1 c_{2\downarrow}^+ c_{1\downarrow} 3 \rangle = 1$
$\langle 1 c_{1\uparrow}^+ c_{2\uparrow} 4 \rangle = 1$	$\langle 2 c_{1\downarrow}^+ c_{1\downarrow} 2 \rangle = 1$	$\langle 2 c_{2\uparrow}^+ c_{2\uparrow} 2 \rangle = 1$
$\langle 2 c_{2\uparrow}^+ c_{1\uparrow} 3 \rangle = -1$	$\langle 2 c_{1\downarrow}^+ c_{2\downarrow} 4 \rangle = -1$	$\langle 3 c_{1\downarrow}^+ c_{2\downarrow} 1 \rangle = 1$
$\langle 3 c_{1\uparrow}^+ c_{2\uparrow} 2 \rangle = -1$	$\langle 3 c_{1\uparrow}^+ c_{1\uparrow} 3 \rangle = 1$	$\langle 3 c_{1\downarrow}^+ c_{1\downarrow} 3 \rangle = 1$
$\langle 4 c_{2\uparrow}^+ c_{1\uparrow} 1 \rangle = 1$	$\langle 4 c_{2\downarrow}^+ c_{1\downarrow} 2 \rangle = -1$	$\langle 4 c_{2\uparrow}^+ c_{2\uparrow} 4 \rangle = 1$
	$\langle 4 c_{2\downarrow}^+ c_{2\downarrow} 4 \rangle = 1$	

Inserting the results from Table 1 together with the expansions in equations (17) to (20) into the total matrix element results, after some algebra, in

$$\begin{aligned}
\langle v_1 | \hat{\rho}(r') | v_2 \rangle &= (-y \langle 1 | + y \langle 2 | + x \langle 3 | + x \langle 4 |) \hat{\rho}(r') \left(\frac{1}{\sqrt{2}} | 1 \rangle + \frac{1}{\sqrt{2}} | 2 \rangle \right) \\
&= \frac{1}{\sqrt{2}} y [-\phi_1 \phi_1 + \phi_1 \phi_1 + \phi_2 \phi_2 - \phi_2 \phi_2] \\
&\quad + \frac{1}{\sqrt{2}} x [-\phi_1 \phi_2 + \phi_1 \phi_2 + \phi_1 \phi_2 - \phi_1 \phi_2] = 0 \\
\langle v_2 | \hat{\rho}(r) | v_1 \rangle &= 0 \\
\langle v_1 | \hat{\rho}(r') | v_3 \rangle &= (-y \langle 1 | + y \langle 2 | + x \langle 3 | + x \langle 4 |) \hat{\rho}(r') \left(\frac{1}{\sqrt{2}} | 3 \rangle - \frac{1}{\sqrt{2}} | 4 \rangle \right) \\
&= \sqrt{2} x [\phi_1(r') \phi_1(r') - \phi_2(r') \phi_2(r')] \\
\langle v_3 | \hat{\rho}(r) | v_1 \rangle &= \sqrt{2} x [\phi_1(r) \phi_1(r) - \phi_2(r) \phi_2(r)]
\end{aligned}$$

$$\begin{aligned}
\langle v_1 | \hat{\rho}(r') | v_4 \rangle &= (-y \langle 1 | + y \langle 2 | + x \langle 3 | + x \langle 4 |) \hat{\rho}(r') (x |1\rangle - x |2\rangle + y |3\rangle + y |4\rangle) \\
&= 4(x^2 - y^2) \phi_1(r') \phi_2(r') \\
\langle v_4 | \hat{\rho}(r) | v_1 \rangle &= 4(x^2 - y^2) \phi_1(r) \phi_2(r)
\end{aligned}$$

Inserting the matrix elements in equation (5) gives the response function for the one-orbital case to be

$$\begin{aligned}
R(r, r'; \omega) &= 16(x^2 - y^2)^2 \phi_1(r) \phi_2(r) \phi_1(r') \phi_2(r') \left[\frac{1}{\omega - \epsilon_4 + \epsilon_1 + i\eta} - \frac{1}{\omega + \epsilon_4 - \epsilon_1 - i\eta} \right] \\
&+ 2x^2 [\phi_1(r) \phi_1(r) \phi_1(r') \phi_1(r') - \phi_2(r) \phi_2(r) \phi_1(r') \phi_1(r')] \\
&- \phi_1(r) \phi_1(r) \phi_2(r') \phi_2(r') + \phi_2(r) \phi_2(r) \phi_2(r') \phi_2(r')] \times \\
&\times \left[\frac{1}{\omega - \epsilon_3 + \epsilon_1 + i\eta} - \frac{1}{\omega + \epsilon_3 - \epsilon_1 - i\eta} \right]
\end{aligned}$$

To find the spectral function of the R_{1111} and R_{2222} terms it can be noted that $\text{Im}\{R_{1111}(\omega)\} = \text{Im}\{R_{2222}(\omega)\} = -2\pi x^2 \delta(\omega - (\epsilon_3 - \epsilon_1))$. Introducing a broadening will cause the spectral function to have peaks at the excitation energy $\Delta\epsilon = \epsilon_3 - \epsilon_1$. The f-sum rule in equation (8) can be calculated analytically using the relationship between $S(\omega)$ and $\text{Im}\{R(\omega)\}$ in equation (6)

$$\int d\omega S(\omega) \omega \propto 2x^2(\epsilon_3 - \epsilon_1) = \frac{8}{16 + (U_0 + \sqrt{U_0^2 + 16})^2} (U_0 + \sqrt{U_0^2 + 16}) \quad (22)$$

disregarding the proportionality constants which will be the same as those for RPA.

2.5 Exact solution for RPA

The RPA polarisation function P^0 is calculated in a non-interacting system as stated in section 2.3. The Hamiltonian used to calculate the eigenenergies and eigenstates used within the RPA is therefore, for this case, reduced to

$$H = \begin{pmatrix} \epsilon_0 & t \\ t & \epsilon_0 \end{pmatrix}$$

Solving the eigenvalue problem two states are found; $\phi_B(r) = 1/\sqrt{2}(\phi_1(r) + \phi_2(r))$, the bonding state with energy $\epsilon_B = \epsilon_0 - t$, and $\phi_A(r) = 1/\sqrt{2}(\phi_1(r) - \phi_2(r))$, the anti-bonding state with energy $\epsilon_A = \epsilon_0 + t$ with a splitting between them equal to $\Delta_0 = \epsilon_A - \epsilon_B = 2t$. The system is assumed to be in the ground state and both electrons are therefore found in

the bonding state. The non-interacting Green's function, equation (12), for the one-orbital case then becomes

$$G^0(r, r'; \omega) = \frac{\phi_B(r)\phi_B^*(r')}{\omega - \varepsilon_B - i\eta} + \frac{\phi_A(r)\phi_A^*(r')}{\omega - \varepsilon_A + i\eta},$$

as only ϕ_B is occupied, whereupon the polarisation function, equation (11), can be written

$$P^0(r, r'; \omega) = -2i \int \frac{d\omega'}{2\pi} \left[\frac{\phi_B(r)\phi_B^*(r')}{\omega + \omega' - \varepsilon_B - i\eta} + \frac{\phi_A(r)\phi_A^*(r')}{\omega + \omega' - \varepsilon_A + i\eta} \right] \\ \times \left[\frac{\phi_B(r')\phi_B^*(r)}{\omega' - \varepsilon_B - i\eta} + \frac{\phi_A(r')\phi_A^*(r)}{\omega' - \varepsilon_A + i\eta} \right].$$

The polarisation function can be seen to take the form

$$\int d\omega' (\alpha + \beta)(\gamma + \kappa) = \int d\omega' (\alpha\gamma + \alpha\kappa + \beta\gamma + \beta\kappa)$$

which can be solved using contour integration. For the $\alpha\gamma$ and $\beta\kappa$ terms the integrals vanish by Cauchy's integral theorem as both have poles only in one of the half-planes. The $\alpha\kappa$ term has a pole in each half-plane and choosing a contour in the upper one and using the Residue theorem for a pole at $\omega' = -\omega + \varepsilon_B + i\delta$ gives $\int d\omega' \alpha\kappa = -2\pi i / (\omega + \Delta_0 - 2i\eta)$. Similarly for $\beta\gamma$ the integral becomes $\int d\omega' \beta\gamma = 2\pi i / (\omega - \Delta_0 + 2i\eta)$. Inserting back the integrals gives

$$P^0(r, r'; \omega) = \phi_A(r)\phi_A(r') \left[\frac{2}{\omega - \Delta_0 + i\eta} - \frac{2}{\omega + \Delta_0 - i\eta} \right] \phi_B(r')\phi_B(r) \quad (23)$$

using that the orbital wave functions are real. From equation (16) it is clear that R^{RPA} must have the same form as P^0 , that is $R^{\text{RPA}} = \phi_A(r)\phi_A(r')R_\omega\phi_B(r')\phi_B(r)$. The RPA equation can then be solved as

$$R^{\text{RPA}} = \phi_A(r)\phi_A(r')P_\omega^0\phi_B(r')\phi_B(r) + \\ + \int dr_1 dr_2 \phi_A(r)\phi_A(r_1)\phi_B(r)\phi_B(r_1)P_\omega^0 v(r_1 - r_2)R_\omega\phi_A(r_2)\phi_A(r')\phi_B(r_2)\phi_B(r') \\ = \phi_A(r)\phi_A(r')[P_\omega^0 + P_\omega^0 R_\omega \langle v \rangle] \phi_B(r')\phi_B(r)$$

where $\langle v \rangle = \int dr_1 dr_2 \phi_A(r_1)\phi_A(r_2)\phi_B(r_1)\phi_B(r_2)$. Consequently, the RPA equation can be written as $R_\omega = P_\omega^0 + P_\omega^0 R_\omega \langle v \rangle$ giving

$$R_\omega = \frac{P_\omega^0}{1 - P_\omega^0 \langle v \rangle}. \quad (24)$$

The result can finally be written as, after some algebra,

$$R_\omega = \frac{\alpha}{\omega - \Delta + i\eta} - \frac{\alpha}{\omega + \Delta - i\eta} \quad (25)$$

with $\Delta = \sqrt{\Delta_0 + 4\Delta_0 \langle v \rangle}$ and $\alpha = 2\Delta_0/\Delta$. The response function within RPA has hence been found to be, expanding $\phi_{A,B}$ into $\phi_{1,2}$,

$$\begin{aligned} R^{RPA}(r, r'; \omega) = & \frac{1}{4} \left[\frac{\alpha}{\omega - \Delta + i\eta} - \frac{\alpha}{\omega + \Delta - i\eta} \right] \cdot [\phi_1(r)\phi_1(r)\phi_1(r')\phi_1(r') \\ & - \phi_1(r)\phi_1(r)\phi_2(r')\phi_2(r') - \phi_2(r)\phi_2(r)\phi_1(r')\phi_1(r') + \phi_2(r)\phi_2(r)\phi_2(r')\phi_2(r')]. \end{aligned}$$

Furthermore, $\langle v \rangle$ can be related to U_0 using that

$$\begin{aligned} \langle v \rangle = & \frac{1}{4} \int dr dr' [\phi_1(r)\phi_1(r)\phi_1(r')\phi_1(r') - \phi_1(r)\phi_1(r)\phi_2(r')\phi_2(r') \\ & - \phi_2(r)\phi_2(r)\phi_1(r')\phi_1(r') + \phi_2(r)\phi_2(r)\phi_2(r')\phi_2(r')] v(r - r') \end{aligned}$$

The $\phi_1(r)\phi_1(r)\phi_2(r')\phi_2(r')$ and $\phi_2(r)\phi_2(r)\phi_1(r')\phi_1(r')$ terms corresponds to inter-site interaction which is not accounted for within the model leaving only the two on-site interaction terms. Each of these can in turn be identified as the U_0 parameter resulting in $\langle v \rangle = \frac{1}{2}U_0$.

Similarly as for R , the RPA spectral functions for R_{1111}^{RPA} and R_{2222}^{RPA} are given using $\text{Im}\{R_{1111}^{RPA}\} = \text{Im}\{R_{2222}^{RPA}\} = -\pi\alpha\delta(\omega - \Delta)/4$ and introducing a broadening causes a peak at the excitation energy Δ . The f-sum rule, equation (8), can also be calculated within RPA again using the relationship between $S(\omega)$ and $\text{Im}\{R(\omega)\}$ in equation (6)

$$\int d\omega S(\omega)\omega \propto \frac{\alpha\Delta}{4} = t = 1 \quad (26)$$

which has no U_0 dependence like the exact result does.

2.6 Numerical solution of R

Even for 2 electrons in the singlet configuration the two orbital per site system is too complicated to be solved analytically. Therefore, a numerical approach was taken to solve the problem. The basis states are for this case defined as $|\text{Orbital 1} \cdot \text{Orbital 2} \cdot \text{Orbital 3} \cdot \text{Orbital 4}\rangle$, i.e. the occupied orbital is the number of dots to the left plus one. Here orbital 1 and 2 are

the lower ones and 3 and 4 the upper, and the basis states are:

$$\begin{aligned}
|1\rangle &= c_{1\uparrow}^+ c_{1\downarrow}^+ |0\rangle = |\uparrow\downarrow\cdots\rangle & |2\rangle &= c_{1\uparrow}^+ c_{2\downarrow}^+ |0\rangle = |\uparrow\cdot\downarrow\cdots\rangle & |3\rangle &= c_{1\uparrow}^+ c_{3\downarrow}^+ |0\rangle = |\uparrow\cdots\downarrow\cdot\rangle \\
|4\rangle &= c_{1\uparrow}^+ c_{4\downarrow}^+ |0\rangle = |\uparrow\cdots\downarrow\rangle & |5\rangle &= c_{1\downarrow}^+ c_{2\uparrow}^+ |0\rangle = |\downarrow\cdot\uparrow\cdots\rangle & |6\rangle &= c_{2\uparrow}^+ c_{2\downarrow}^+ |0\rangle = |\cdot\uparrow\downarrow\cdots\rangle \\
|7\rangle &= c_{2\uparrow}^+ c_{3\downarrow}^+ |0\rangle = |\cdot\uparrow\cdot\downarrow\cdot\rangle & |8\rangle &= c_{2\uparrow}^+ c_{4\downarrow}^+ |0\rangle = |\cdot\uparrow\cdots\downarrow\rangle & |9\rangle &= c_{1\downarrow}^+ c_{3\uparrow}^+ |0\rangle = |\downarrow\cdots\uparrow\cdot\rangle \\
|10\rangle &= c_{2\downarrow}^+ c_{3\uparrow}^+ |0\rangle = |\cdot\downarrow\cdot\uparrow\cdot\rangle & |11\rangle &= c_{3\uparrow}^+ c_{3\downarrow}^+ |0\rangle = |\cdots\uparrow\downarrow\cdot\rangle & |12\rangle &= c_{3\uparrow}^+ c_{4\downarrow}^+ |0\rangle = |\cdots\uparrow\cdot\downarrow\rangle \\
|13\rangle &= c_{1\downarrow}^+ c_{4\uparrow}^+ |0\rangle = |\downarrow\cdots\uparrow\rangle & |14\rangle &= c_{2\downarrow}^+ c_{4\uparrow}^+ |0\rangle = |\cdot\downarrow\cdots\uparrow\rangle & |15\rangle &= c_{3\downarrow}^+ c_{4\uparrow}^+ |0\rangle = |\cdots\downarrow\cdot\uparrow\rangle \\
|16\rangle & & |16\rangle &= c_{4\uparrow}^+ c_{4\downarrow}^+ |0\rangle = |\cdots\uparrow\downarrow\rangle & &
\end{aligned}$$

A code was produced to solve the matrix elements $\langle k | c_i^+ c_j | l \rangle$ stepwise. First operations of the form $c_j | l \rangle$ are performed on the array entries containing the occupation numbers representing the states $|1\rangle$ to $|16\rangle$; as c_i and c_j^+ are Hermitian conjugates the operations are also valid for $\langle k | c_i^+$. The remaining occupation number after the annihilation operation is stored together with the sign resulting from the operation based on the anticommutation relation $\{c_i^+, c_j\} = \delta_{ij}$ and the ordering convention of the operators as defined in appendix A. After the annihilation operations, the matrix elements have reduced to the form $\langle 0 | c_m c_n^+ | 0 \rangle$ whence it becomes clear that $m = n$ for a non-zero element with the resulting sign being the product of the signs calculated in the previous step.

The calculated matrix elements can then be used to acquire the 16×16 Hamiltonian of the problem using equation (3). As stated in section 2.1 the terms which will be considered are $h_{11} = h_{22} = \varepsilon_0$, $h_{33} = h_{44} = \varepsilon_1$, $t_{12} = t_{21} = t$, $t_{14} = t_{41} = t_{23} = t_{32} = t'$, and $U_{1111} = U_{2222} = U_0$ and constitutes the parameters of the problem. The Hamiltonian is diagonalized using the *LAPACK* [8] subroutine *dsyev* giving the eigenenergies and eigenstates.

Then the $\langle \Psi | \hat{\rho}(r') | n \rangle$ and $\langle n | \hat{\rho}(r) | \Psi \rangle$ matrix elements in the response function are calculated using the matrix elements between the basis states and the expansion coefficients for $|\Psi\rangle$ and $|n\rangle$ from the diagonalization. The final response function is subsequently calculated as R_{ijkl} matrix elements, corresponding to the $\phi_i(r)\phi_j(r)\phi_k(r')\phi_l(r')$ terms.

2.7 Numerical solution for RPA

The non-interacting Hamiltonian in the two-orbital case is found by making a mean-field approximation for each of the electrons. For the spin up electron the field which acts upon it will arise from the mean occupation number of the spin down electron on that orbital, that is to say the expectation value $\langle n_{i\downarrow} \rangle$ taken in the ground state which is assumed to only have occupation in the lower orbitals as no Coulomb interaction occurs for the upper. The expectation value then becomes

$$\langle n_{i\downarrow} \rangle = \langle \Psi | n_{i\downarrow} | \Psi \rangle = \left(\sum_{k=1}^2 b_k \langle k | \right) n_{i\downarrow} \left(\sum_{l=1}^2 b_l | l \rangle \right) = \sum_{k,l=1}^2 b_k b_l \langle k | n_{i\downarrow} | l \rangle$$

where b_k is the real expansion coefficient of the ground state in the basis state $|k\rangle$. The resulting Hamiltonian can be written

$$H = \sum_{i,j} \sum_{\sigma} h_{ij} c_{i\sigma}^{\dagger} c_{j\sigma} + \sum_i U_{iiii} n_{i\uparrow} \langle n_{i\downarrow} \rangle = \sum_{i,j} \sum_{\sigma} h_{ij} c_{i\sigma}^{\dagger} c_{j\sigma} + \sum_i U_0 (n_{i\uparrow} b_1^2 + n_{i\downarrow} b_2^2). \quad (27)$$

which in matrix form is

$$H = \begin{pmatrix} \epsilon_0 + b_1^2 U_0 & t & 0 & t' \\ t & \epsilon_0 + b_2^2 U_0 & t' & 0 \\ 0 & t' & \epsilon_1 & 0 \\ t' & 0 & 0 & \epsilon_1 \end{pmatrix}$$

The same also holds for the spin down electron. To find the eigenvalues and eigenstates the problem is solved self-consistently with respect to the expansion coefficients b_1 and b_2 with the initial guess of equal probability in the lower states. When the differences $|b_{1\text{new}} - b_{1\text{old}}|$ and $|b_{2\text{new}} - b_{2\text{old}}|$ becomes smaller than a chosen threshold value the process is terminated. To ensure convergence the diagonalization using *dsyev* in *LAPACK* [8] is carried out using a mixing between the old and new states as $b_{i\text{mix}} = (1 - x)b_{i\text{old}} + xb_{i\text{new}}$ with $x = 0.1$ being a small mixing parameter.

Using the expansions of the eigenstates in the basis orbitals ϕ_i obtained from the diagonalization, P^0 in equation (13) can be written as

$$P^0(r, r'; \omega) = \sum_i^{\text{occ}} \sum_j^{\text{unocc}} \sum_{\alpha, \beta, \gamma, \kappa} b_{\alpha}^i \phi_{\alpha}(r) b_{\beta}^j \phi_{\beta}(r) b_{\gamma}^i \phi_{\gamma}(r') b_{\kappa}^j \phi_{\kappa}(r') \left[\frac{1}{\omega - \epsilon_j + \epsilon_i + i\eta} - \frac{1}{\omega + \epsilon_j - \epsilon_i - i\eta} \right]. \quad (28)$$

where $\alpha, \beta, \gamma, \kappa$ give the orbitals. As such P^0 can be regarded as a 16×16 array with elements $P_{(\alpha\beta),(\gamma\kappa)}^0$

$$P_{(\alpha\beta),(\gamma\kappa)}^0 = b_{\alpha}^i b_{\beta}^j b_{\gamma}^i b_{\kappa}^j \left[\frac{1}{\omega - \epsilon_j + \epsilon_i + i\eta} - \frac{1}{\omega + \epsilon_j - \epsilon_i - i\eta} \right]. \quad (29)$$

Noticing that R^{RPA} must have the same form in the RPA equation it can be shown in a similar way as done in section 2.5 that the RPA equation becomes

$$R_{(\alpha\beta),(\gamma\kappa)}(\omega) = P_{(\alpha\beta),(\gamma\kappa)}^0(\omega) + \sum_{\alpha'\beta'\gamma'\kappa'} P_{(\alpha\beta),(\gamma'\kappa')}^0(\omega) V_{(\alpha'\beta'),(\gamma'\kappa')} R_{(\gamma'\kappa'),(\gamma\kappa)}(\omega) \quad (30)$$

which can be identified as a matrix equation

$$[R^{\text{RPA}}] = [P^0] + [P^0][V][R^{\text{RPA}}] \quad (31)$$

where the non-zero entries of $[V]$ are the ones corresponding to two electrons occupying the same lower orbital. These are the diagonal elements $\alpha = \beta = \gamma = \kappa = 1, 2$. The matrix equation can be solved for $[R^{\text{RPA}}]$ giving

$$[R^{\text{RPA}}] = [I - [P^0][V]]^{-1} [P^0] \quad (32)$$

Carrying out the matrix multiplications and using the subroutine *zgetri* in *LAPACK* to find the inverse provides the matrix elements $R_{(\alpha\beta),(\gamma\kappa)}^{\text{RPA}}$ which can be compared to the ones calculated in section 2.6 for the response function: R_{ijkl} .

3 Results

In the following all parameters are given in units of the hopping term $t = 1$ and the Figures are plotted using *MATLAB* [9].

3.1 One-orbital

For the one-orbital case the spectral function matrix elements $S_{1111} + S_{2222}$ for both the exact solution of the response function and that within RPA can be seen in Figure 1 for $U_0 = 0.2, 1$ and 4 plotted with an introduced Lorentzian broadening. It is clearly visible that a given U_0 causes the excitation energy, given by the peak, within the RPA to deviate from the exact solution.

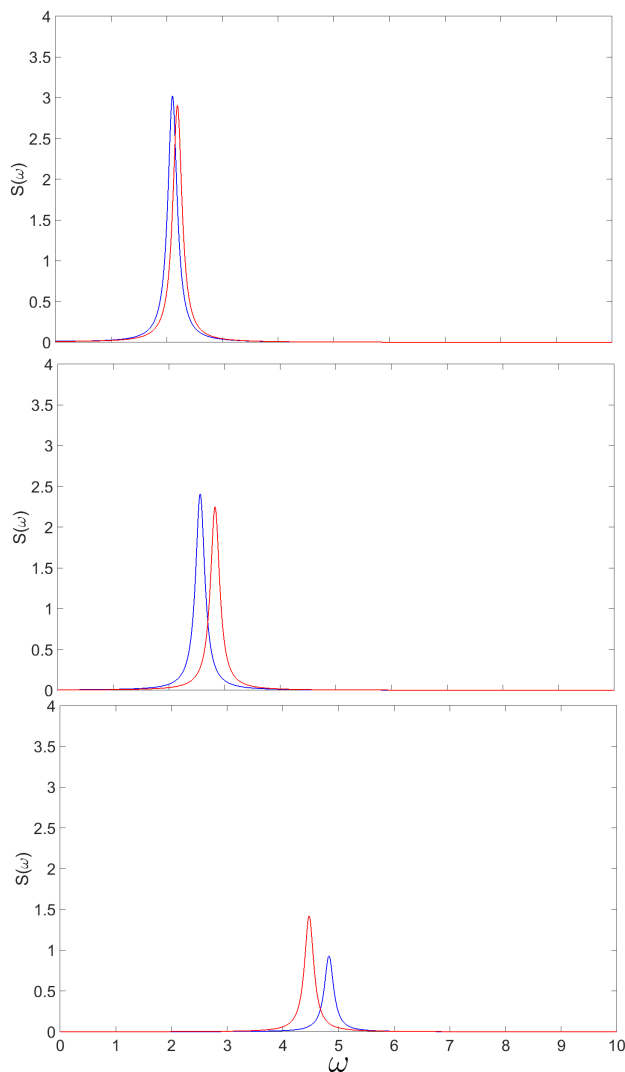


Figure 1: The exact (blue) and RPA (red) spectral function matrix elements $S_{1111} + S_{2222}$ with $t = 1$ for $U_0 = 0.2, 1$ and 4 from top to bottom for the one-orbital case.

For larger and larger U_0 the trend is that RPA underestimates the energy, however, as can be seen RPA overestimates for small U_0 and there should therefore be a range for which the exact solution and RPA gives a similar result. This can be identified by equating the excitation energies of the exact solution, $\epsilon_4 - \epsilon_2 = 1/2(U_0 + \sqrt{U_0^2 + 16t^2})$, and that of RPA, $\Delta = \sqrt{2t + 4tU_0}$. The result can be seen plotted in Figure 2 showing an exact agreement for $U_0 = 0$ and $U_0 = 3$. The f-sum rule computed in equations (22) and (26) can be seen plotted in Figure 3 and shows that the best fit between RPA and the exact response function is for small U_0 .

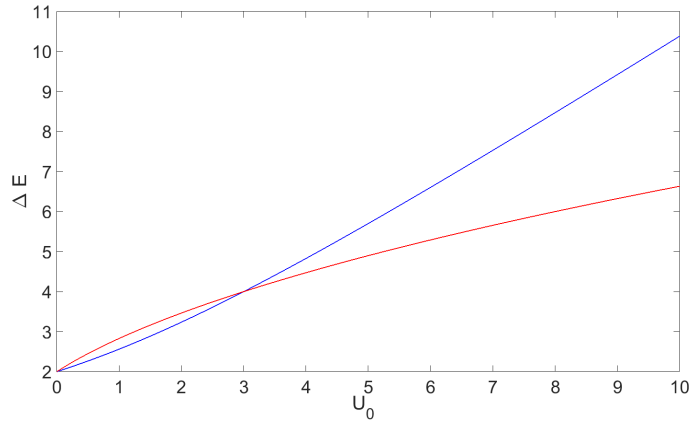


Figure 2: Excitation energy for the exact solution (blue) and RPA (red) for the one-orbital case plotted as a function of the parameter U_0 .

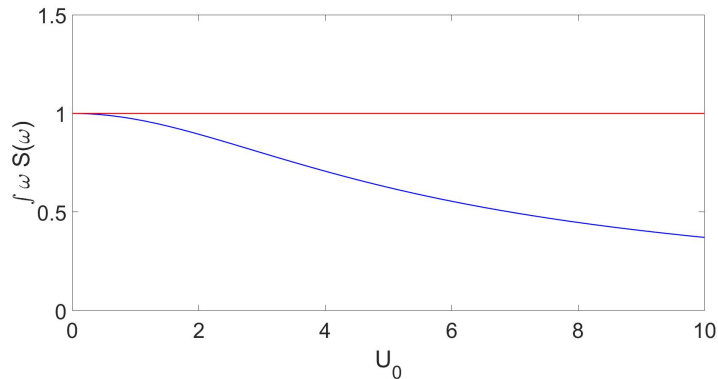


Figure 3: The f-sum rule calculated for the exact solution (blue) and RPA (red) for the one-orbital case plotted as a function of the parameter U_0 .

3.2 Two-orbital

For the two-orbital case there are three possible parameters to vary, ϵ_1 , U_0 and t' , so in order to be able to discern trends and the influence of a given parameter one of the three is varied

with the other two being kept fixed at a time. It should also be noted that the plotted values are given for $S_{1111} + S_{2222}$ if not otherwise stated and the broadenings are Lorentzian.

U_0 is varied in Figure 4 for fixed $\epsilon_1 = 2$ and $t' = 0.5$. Increasing U_0 seems to have the overall effect of decreasing the agreement between RPA and the exact solution; although, for a given set of parameters some excitation energies agree well for $U_0 = 4$ while there are others which do not, or are not present in the RPA altogether. There seems to be at most three peaks within RPA while the exact solution is not limited to this number. For this reason the imaginary part of P_{1111}^0 and R_{1111}^{RPA} are plotted in Figure 5 (c) for $\epsilon_1 = 2$, $U_0 = 1$ and $t' = 1$ in order to try and identify the origin of the excitations.

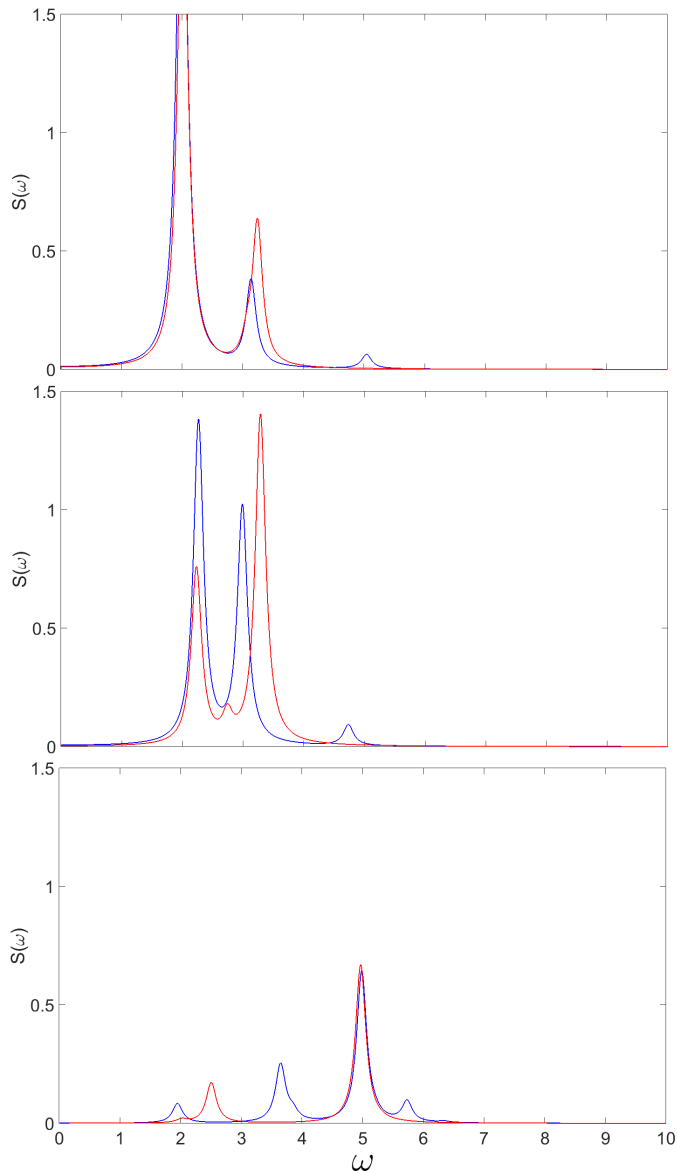


Figure 4: The exact (blue) and RPA (red) spectral function matrix elements $S_{1111} + S_{2222}$ with $\epsilon_1 = 2$ and $t' = 0.5$ for $U_0 = 0.2, 1$ and 4 from top to bottom for the two-orbital case.

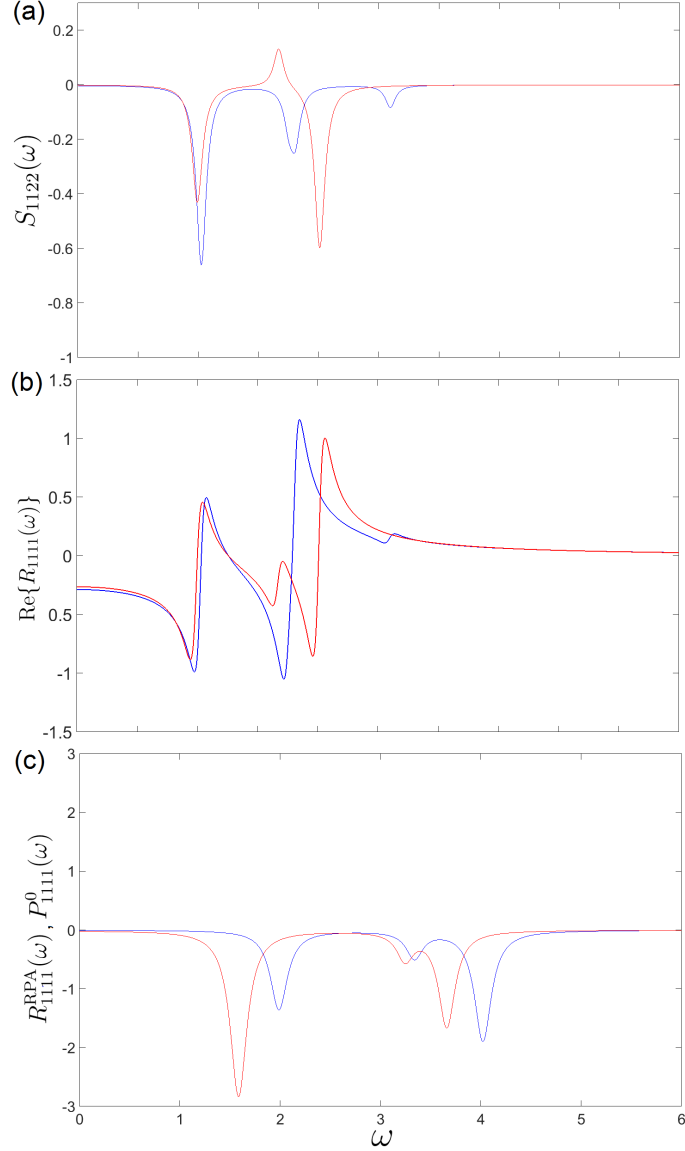


Figure 5: The plots are for the two-orbital case with $\epsilon_1 = 2$, $U_0 = 1$ and $t' = 1$ and shows (a): The exact (blue) and RPA (red) spectral function off-diagonal matrix element S_{1122} . (b): The exact (blue) and RPA (red) real part of matrix element R_{1111} . (c): The imaginary parts of the R_{1111}^{RPA} (blue) and P_{1111}^0 (red) matrix elements.

In Figure 6 t' is varied while $\epsilon_1 = 2$ and $U_0 = 1$ are kept fixed. The general trend for these spectra is that an increase in t' seems to improve the coherency between RPA and the exact result. This becomes more evident when varying t' for a larger $U_0 = 6$ as can be seen in Figure 7. Even for a relatively large U_0 which by the previous results should worsen the agreement the large t' seems to have a mitigating effect albeit it does not make it perfect as the exact result has several peaks missing in RPA. Furthermore, when decreasing t' towards 0 the trend is that the excitation spectrum seems to revert back to the one-orbital case.

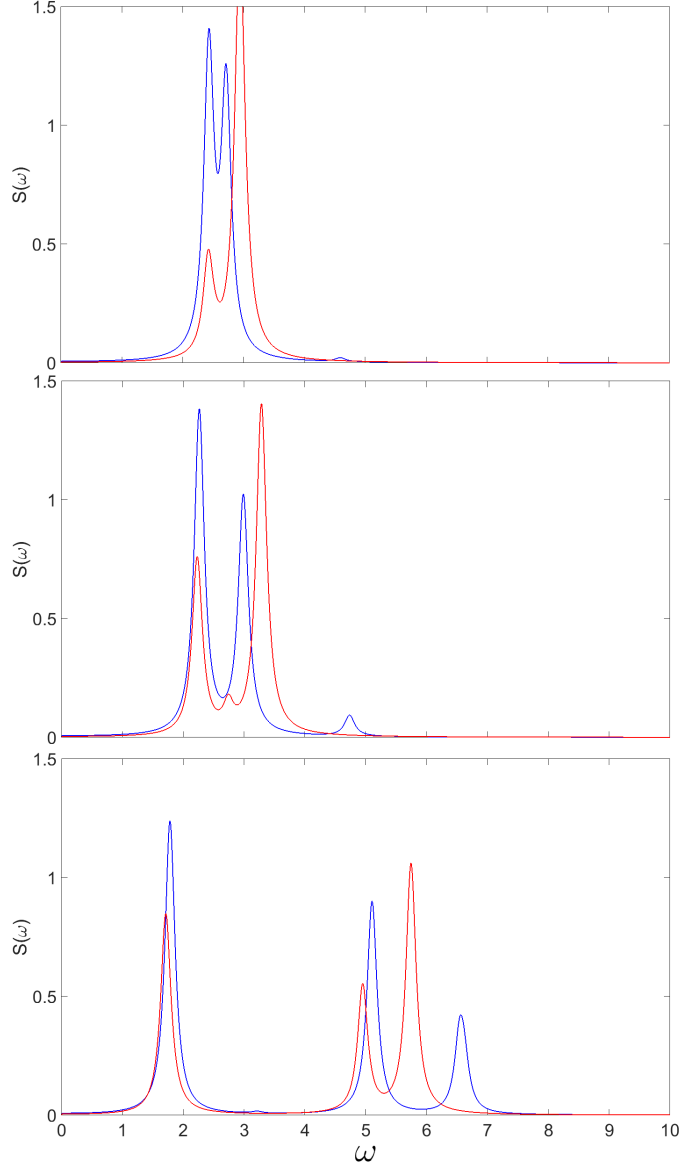


Figure 6: The exact (blue) and RPA (red) spectral function matrix elements $S_{1111} + S_{2222}$ with $\epsilon_1 = 2$ and $U_0 = 1$ for $t' = 0.2, 0.5$ and 2 from top to bottom for the two-orbital case.

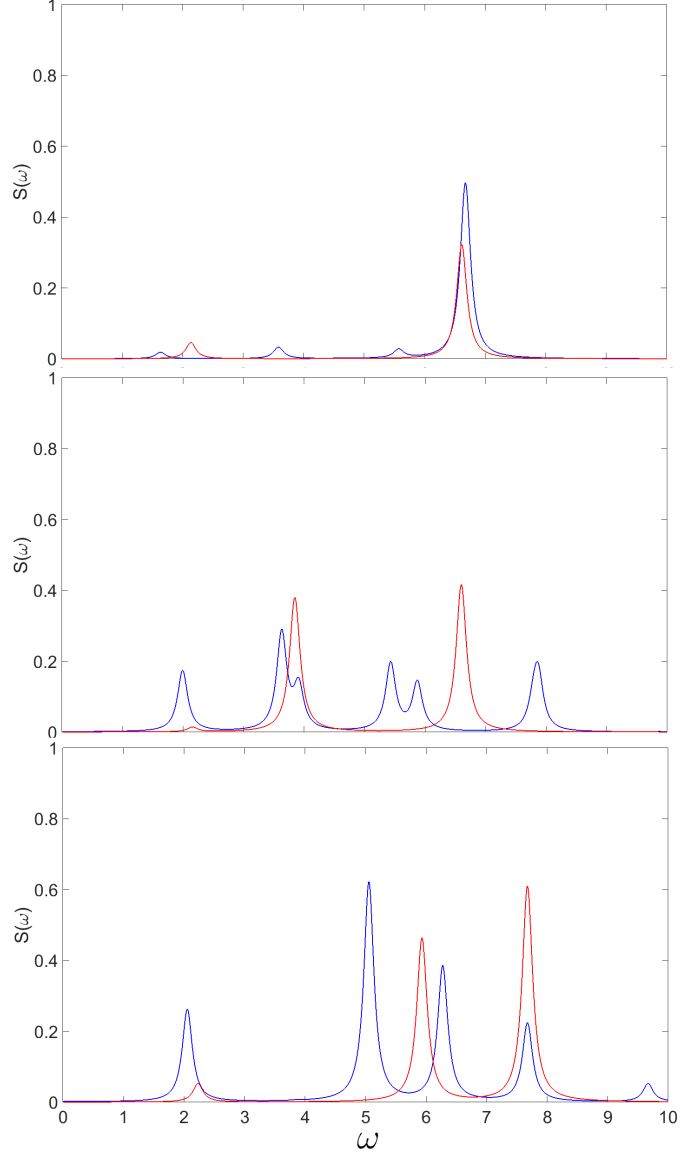


Figure 7: The exact (blue) and RPA (red) spectral function matrix elements $S_{1111} + S_{2222}$ with $\epsilon_1 = 2$ and $U_0 = 6$ for $t' = 0.2, 1$ and 2 for the two-orbital case.

The remaining parameter to vary, ϵ_1 , seems to revert the system back to the one-orbital case when instead increased as can be seen from Figure 8 with $U_0 = 1$ and $t' = 0.5$ fixed. In addition, the spectra also seems to get less affected with respect to changing U_0 and t' for a large ϵ_1 .

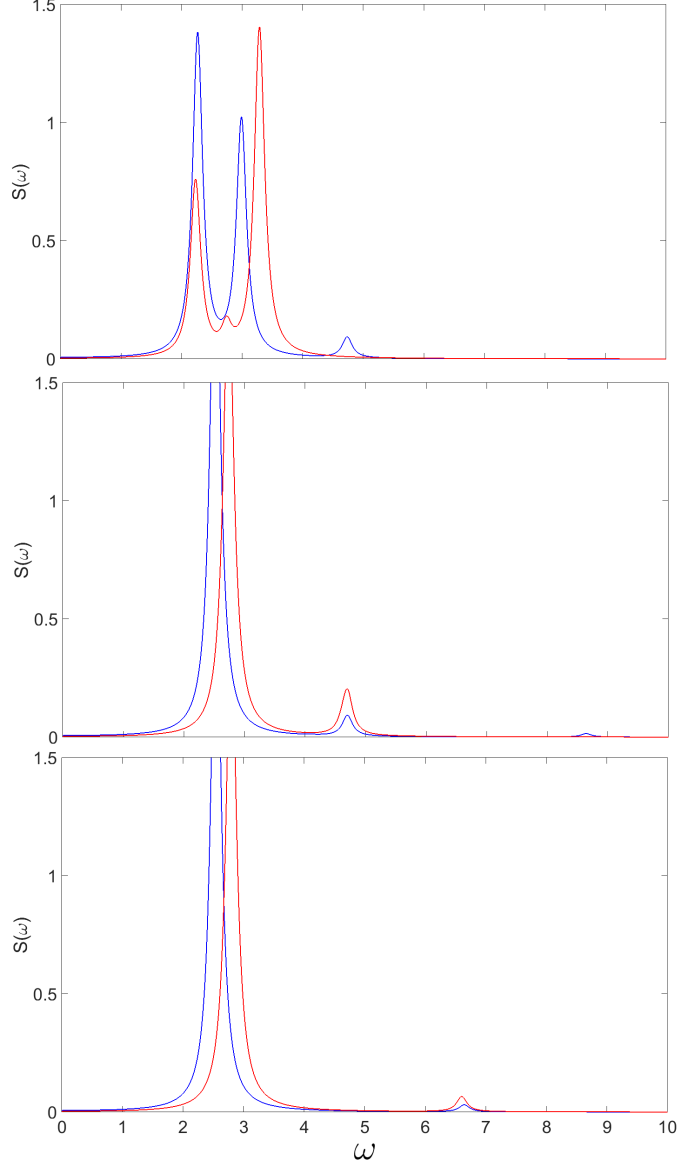


Figure 8: The exact (blue) and RPA (red) spectral function matrix elements $S_{1111} + S_{2222}$ with $U_0 = 1$ and $t' = 0.5$ for $\epsilon_1 = 2, 4$ and 6 for the two-orbital case.

For comparison also the off-diagonal matrix element S_{1122} for $\epsilon_1 = 2$, $U_0 = 1$ and $t' = 1$ are shown in Figure 5 (a) and the real part of R_{1111} in (b). The real part can be seen to change sign whenever there is an excitation. By numerically integrating the spectral function as in equation (8) how well the f-sum rule concur for $S_{1111} + S_{2222}$ and $S_{1111}^{\text{RPA}} + S_{2222}^{\text{RPA}}$ can be tested using a cut-off of $\omega = 10$. The result is consistent with the previous trends that for a large U_0 RPA deviates from the exact one and a larger t' improves the agreement.

It should also be noted that the $S_{3333} + S_{4444}$ spectra gives the same excitation energies as $S_{1111} + S_{2222}$ but different, and in general weaker, strengths.

4 Conclusion

It should be noted that the model used in this work is of a limited scope and the results may therefore not be fully applicable to a real case except perhaps qualitatively. It is, however, previously known that RPA fails in the domain of large U_0 for real materials and this behavior is also present for the current model. U_0 is measured in units of t and it therefore gives a measure of the strength of correlations in the system as for high U_0 it is unfavorable for two electrons to be on the same orbital. This causes them to localize, giving a correlation between their positions.

For the one-orbital case it can be seen that the agreement is relatively good up to around $U_0 = 4$, as compared to even larger U_0 , which is a lot larger than the hopping $t = 1$ and might therefore by the previous discussion be thought to give an erroneous match. The reason for this is due to the fact that RPA first overestimates the excitation energy for small U_0 and then underestimates it for large U_0 giving the "coincidence" of a good agreement also for larger U_0 as can be seen in Figure 2.

This behavior can also help to explain why, in the two-orbital case, the agreement between RPA and the exact response for some excitation peaks seems to improve also for larger U_0 which can be seen, for example, for the second highest excitation energy in Figure 4 as a crossing between the exact result and RPA. That not the entire spectrum is in agreement for some value of U_0 , as it is for the one-orbital case with $U_0 = 3t$, can probably be explained by the more complex case arising from also allowing hopping to the higher orbitals, which gives rise to other causes of the excitations.

The trend that a large t' gives an improved result for RPA can also be linked to the case of delocalization as for U_0 . The delocalization effect of t' is, however, instead caused by allowing the electrons to occupy a larger space through the increase in probability of hopping to the higher states. This can be likened to the case of the electron gas; for a high density the electrons are highly delocalized as they are unable to avoid each other, causing localization to be less important. As such the system can be considered delocalized for which it is known that RPA is good. This is in agreement with the obtained results. Also in real materials in cases where RPA is good this could provide an explanation since there are many excited states giving a larger t' .

The reversion back to the one-orbital case for small t' can also be explained in terms of the hopping between the lower and upper states; for a small t' the probability for an electron to go from the lower orbitals to the upper is small and when t' tends to zero the two orbitals will be completely separated. Thus applying some external field to the system will cause the electrons to only move in the lower orbitals providing the response of the one-orbital system.

Also for increasing ϵ_1 the trend was that the system reverted back to the one-orbital case. Here the explanation instead can be seen from how ϵ_1 in-fact gives the effective gap between the lower and upper orbitals as $\epsilon_0 = 0$. Therefore, increasing ϵ_1 will effectively decrease the hopping strength and, as a consequence, also the probability of an electron to go into the upper orbitals.

By examining Figure 5 (c) it can be seen that all three found peaks for RPA originate from the non-interacting response P^0 . There has therefore not emerged any collective excitations, such as there would in real systems, which otherwise the denominator of equation (24) would be the cause of (strictly speaking, it is in-fact a matrix equation like equation (32)). It is also possible that increasing the number of electrons could have this effect, however, this was not done during this work. This might be a general feature for smaller systems and could be due to the lack of long-range interactions. It is, however, in the present study found that the excitation peaks are shifted relative to the non-interacting ones which would then be caused by the local interactions in the denominator. The number of excitation energies for the exact response, in this case 15, is instead only limited by the number of excited states for the interacting Hamiltonian.

When observing the real part of the response it was noted that the function changed sign whenever there was an excitation peak. This result can be found from equation (7) as $S(r, r'; \omega)$ consists of delta functions giving terms of the form $1/(\omega - (E_n - E_0))$. These terms will be positive for $\Delta E_n = (E_n - E_0)$ less than ω and negative when ΔE_n is larger than ω providing the observed behavior.

Because of the disparity between RPA and the real response function, which abides by the f-sum rule, it can be seen from both the analytical and the numerical examples that RPA does not fulfill the f-sum rule. Indeed, there is no proof that it should fulfill it, however, for real systems RPA seems to do so. This could possibly be explained by the aforementioned delocalization caused by t' which is in agreement with the trend that the f-sum rule was in better agreement for large t' . The trend of a worsening f-sum rule for RPA with increasing U_0 can also be related back to the general deterioration of RPA for large U_0 . It is, however, also possible that a part of the strengths have transferred to the other matrix elements as only $S_{1111} + S_{2222}$ have been considered and the f-sum rule applies to $S(\omega)$.

The reasoning behind plotting $S_{1111} + S_{2222}$ was to make site 1 and 2 interchangeable as for individual elements they gave the same excitation energies but not the same strengths. As the naming convention for the state is arbitrary there should be no difference between placing an electron on the sites which lead to the current choice. The off-diagonal elements can both change sign and have different sign for a given excitation energy for the exact response and RPA, as seen in Figure 5 (a), making it difficult to do a comparison. As such, it was decided

to only analyze the diagonal elements.

The validity of the created program was tested, besides seeing if the two-orbital case reverted back to the one-orbital case for $t' = 0$ and large ϵ_1 , also by comparing the obtained matrix elements with analytically calculated ones such as those in section 2.4. The code can be made available upon request.

5 Outlook

A possible expansion of this work could be to increase the number of orbitals on each site to better resemble a real system, by making alterations to the produced code. The only major changes required are adding additional basis states with the new configurations, to also allow for occupation of higher orbitals, and changing the size of the matrices and loops to account for this, add the additional variables needed for the interacting Hamiltonian, and find the new Hamiltonian within RPA as this was done analytically. The effective model used during this work can thus be studied by downfolding the higher states into a smaller subspace of the Hilbert-space whereupon the Green's function and self-energy can be calculated. This is also done in real systems where the band structure is downfolded into ones around the Fermi level to limit the problem to the region of physical interest.

Another way of continuing would be to try to improve RPA by for example removing the self-interactions arising from the Hartree approximation. This is, however, not a problem for the current model as only the singlet configuration was studied. If instead two same spin electrons had been studied, as could be the case in real systems, self-interaction would occur and would not be canceled since exchange is not taken into account. Also vertex corrections such as electron-hole interactions could be taken into account in the RPA equation.

Appendix A Occupation number representation

This short summary of occupation number representation follows Raimis [10].

Electron wave functions are usually represented as determinantal functions due to their antisymmetric properties from being fermions, where a general determinantal function has the following form

$$\Psi(x_1, \dots, x_n) = \frac{1}{\sqrt{n!}} \begin{vmatrix} \phi_1(x_1) & \cdots & \phi_1(x_n) \\ \vdots & \ddots & \vdots \\ \phi_n(x_1) & \cdots & \phi_n(x_n) \end{vmatrix} \quad (33)$$

Another way of representing the total state of an electronic system is using second quantization, or occupation number representation, wherein only what states are occupied and unoccupied are given. Hence, a definition of the internal positions of the states within the determinant, and therefore also the occupation number ket, is required. The convention which will be used throughout this work is that the positions are ordered by increasing orbital numbers k .

Assuming a system has four possible states, or orbitals, ϕ_1 , ϕ_2 , ϕ_3 and ϕ_4 , the total system can be represented in bra-ket notation as $|n_1 \cdot n_2 \cdot n_3 \cdot n_4\rangle$, where n_i can take either 1 if the corresponding state is occupied or 0 if it is unoccupied.

As spin, σ , is taken into account in the present work a slightly different notation will be used where occupation by a spin up electron is represented by $\sigma = \uparrow$ and a down electron by $\sigma = \downarrow$, giving for the previous system with an up electron occupying ϕ_1 and a down electron occupying ϕ_3 : $|\uparrow \cdot \cdot \downarrow \cdot \rangle$ with the 0 being omitted for simplicity. The inclusion of spin warrants a change of the numbering of states, as $i = (k, \sigma)$, to having \downarrow representing a larger value than \uparrow for a given k .

In order to change occupation numbers annihilation and creation operators are introduced acting on the kets. The annihilation operator, c_i , acts on a state by removing the occupation of an electron in state ϕ_i which corresponds to reducing an N -electron determinantal function to an $N - 1$ by removing ϕ_i from it. If the state does not contain ϕ_i , by definition,

$$c_i |n_1 \cdot n_2 \cdot \dots \cdot n_i = 0 \cdot n_{i+1} \cdot \dots\rangle = 0. \quad (34)$$

Similarly the creation operator c_k^+ acts on the ket by adding an electron to state ϕ_i which corresponds to increasing the N -determinantal function to an $N + 1$ one by adding ϕ_i . Conversely as for the annihilation operator, acting with the creation operator on an already occupied state gives 0. Furthermore, the annihilation and creation operators are Hermitian

conjugates.

Annihilation or creation does not necessarily have to occur in a specific order, however, care has to be taken that the arising sign from the operations is correct due to the real wave function being of the form of a determinant. Using the definition that the operation occurs at the first position an unambiguous sign convention can be chosen as it arises from rearranging the states between their defined positions and the first position in the system.

A vacuum state $|0\rangle$ containing no occupation can also be introduced, to which any state can be reduced to or created from. Using the aforementioned convention of ordering, the previous example can be written as $c_{1\uparrow}^+ c_{3\downarrow}^+ |0\rangle$. This type of notation is useful for finding the sign which arises after operating with the annihilation or creation operator on a state since the anticommutation relations between the operators can be used to rearrange them. These relations are for arbitrary states $i, j = (k, \sigma)$ as follows:

$$\{c_i, c_j\} = 0 \tag{35}$$

$$\{c_i^+, c_j^+\} = 0 \tag{36}$$

$$\{c_i^+, c_j\} = \delta_{ij}. \tag{37}$$

References

- [1] Pines, D., *Elementary excitations in solids*. New York: W.A. Benjamin, Inc. (1963)
- [2] Martin, R., *Electronic structure: basic theory and practical methods*. New York: Cambridge University Press (2010).
- [3] Seitz, F., Turnbull, D., Ehrenreich, H. (eds.), *Solid state physics, volume 23*. New York and London: Academic Press (1969).
- [4] Bohm, D., Pines, D., *A Collective Description of Electron Interactions: III. Coulomb Interactions in a Degenerate Electron Gas*. Phys. Rev. **92**, 609 (1953).
- [5] Gell-Mann, M., Brueckner, K., *Correlation Energy of an Electron Gas at High Density*. Phys. Rev. **106** 364 (1957).
- [6] Kojima, A., et. al., *Organometal Halide Perovskites as Visible-Light Sensitizers for Photovoltaic Cells*. J. Am. Chem. Soc. **131** 6050 (2009).
- [7] Hubbard, J., *Electron correlations in narrow energy bands*. Proc. R. Soc. Lond. A **276** 238 (1963).
- [8] *LAPACK - Linear Algebra PACKage*, Univ. of Tennessee, Univ. of California, Univ. of Colorado, NAG Ltd.. [Cited 2017 May 8]. Available from: <http://www.netlib.org/lapack/>.
- [9] *MATLAB* [Cited 2017 May 8], The MathWorks, Inc.. Available from: <https://se.mathworks.com/products/matlab.html>.
- [10] Raimes, S., *Many-electron theory*. Amsterdam: North-Holland Publishing Company (1972).